

Charged Particle Emissions and Surface Morphology of Pd/PdO:D_x and TiD_x Targets Under Electron Beam Excitation

A. Lipson¹, I. Chernov², V. Sokhoreva², V. Mironchik², A. Roussetski³, A. Tsivadze¹, Y. Cherdantsev², B. Lyakhov¹, E. Saunin¹ and M. Melich⁴

1 A.N. Frumkin Institute of Physical Chemistry and Electrochemistry, Russian Academy of Sciences, Moscow 199915, Russia

2 Tomsk Polytechnic University, Tomsk, 634050 Russia

3 P.N. Lebedev Physics Institute, Russian Academy of Sciences, Moscow, 119991 Russia

4 Naval Postgraduate School, Monterey CA 93943 -5000 USA

E-mail: rusets@x4u.lebedev.ru

Abstract. We report charged particle emission from metal deuterides upon e-beam excitation of their surface. Detection and identification was made using CR-39 plastic track detectors with Cu and Al absorbers. Protons with primary energy 3 MeV and α -particles with energies $E_{\alpha} > 10$ MeV are observed.

1. Introduction

First principles calculations of hydrogen desorption from metal hydrides with a high hydrogen solubility [1], show that excitation of the hydrogen subsystem in those deuterides produces plasmons that create strong electric fields ($F \sim 10^8$ V/cm) on a lattice parameter scale ($a \sim 0.3$ - 0.4 nm). As a result, the mean energy of desorbed protons/deuterons (E_d), escaping from the hydride surface, is increased from $kT(1/40$ eV) to several eV ($E_d = F \times a \sim 3$ - 4 eV) or two orders of magnitude larger, effectively producing “hot” deuterons. Such a deuteron acceleration mechanism, along with a large electron screening, could strongly enhance DD-reaction product yield, even at these extremely low excitation energies.

The purpose of this present study is:

- To verify the hypothesis that excitation of the hydrogen subsystem in metal deuterides enhances DD reaction yield.
- To check feasibility of energetic alpha-particle emission under e-beam irradiation.
- To test a new triple CR-39 detector design in vacuum experiments, allowing charged particle identification

2. Experimental

Three plastic track (noiseless) CR-39 detectors are exposed to deuterated samples being excited by an electron beam. The CR-39 detectors were covered by Al and Cu foils with known stopping ranges (this arrangement can be considered as the simplest dE-E detector without time converter), see Fig.1. The Foreground counts are read out from the CR-39 surface of the detectors facing the sample. The Background counts are read from the rear sides of these same detectors that face either the vacuum chamber or the stainless steel support. The sample-detector holder assembly is mounted in the SEM vacuum chamber ($p = 10^{-6}$ torr) and irradiated by a collimated electron beam ($J = 100$ - 300 nA, $E = 30$ keV). The desorbed deuterium and generated charged particles reach the detectors from the spot produced by e-beam, area $S = 8 \times 6$ mm². The effective distance between the center of the spot and the detectors 1 and 2 is about $\langle R_{eff} \rangle = 12$ mm.

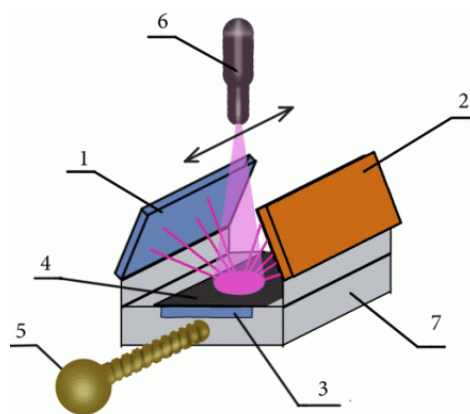


Fig.1. - 1,2 and 3 – are the CR-39 detectors covered with the 11 μm Al (1), 25 μm Cu (2) and 33 μm Al (3) foils, respectively, 4 –deuterated sample, 5-manipulator, 6-electron gun, 7- stainless support

The Landauer CR-39 detectors ($2 \times 1 \text{ cm}^2$) with initial total track density ($N \leq 20 \text{ cm}^{-2}$) were calibrated using a Van De Graaf accelerator (normal incidence protons beams with the energy ranging from 0.6 – 3.0 MeV), a cyclotron α -beam (11 – 30 MeV) and with alpha sources. Calibration functions, track diameter vs. particle energy, were obtained for various CR-39 etching times (Fig.2) or equivalently, depths. Special calibration of CR-39 detectors in a four detector experimental series has also been carried out using extended Pu-238 alpha source placed at the sample position. The calibration showed that overall efficiency of the detectors 1 and 2 is $\epsilon = 2.6 \%$, while the efficiency of the detector #3 is of $\sim 8.0 \%$. Note in these experiments more than 80 % of alpha tracks detected by detectors 1 and 2 have normal incidence.

In reference experiments without e-beam stimulation two CR-39 detectors (no metal cover and one covered with 25 μm Cu) were used to obtain background levels in the SEM.

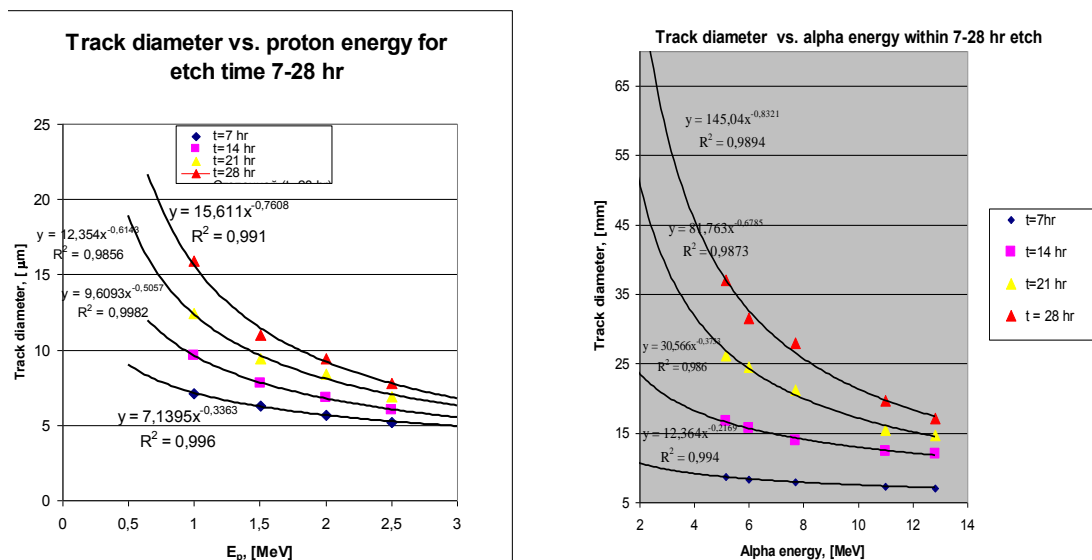


Fig.2. - Landauer CR-39 track diameter vs. charged particle energy (accelerator calibration data) for protons (left) and alphas (right) of normal incidence at various etching time (etching conditions: 6 N NaOH at $t = 70^\circ\text{C}$)

The PdO/Pd/PdO samples are prepared by thermal oxidation of Nilaco (Japan) Pd foil (99.95 % purity), 50 μm thick with area $S = 30 \times 10 \text{ mm}^2$. Electrochemical loading uses 0.3M-LiOD solution in D_2O with Pt anode; $j = 10 \text{ mA/cm}^2$ $T \sim 280 \text{ K}$ (below room temperature) in a special electrolytic cell with separated cathode and anodic spaces. ($x = \text{D/Pd} \sim 0.73$, about 40 min is required). The samples are rinsed in pure D_2O and then placed in liquid nitrogen in a Dewar flask to cool to $T = 77 \text{ K}$. The cooled samples are rapidly mounted (during 1 min) in the sample holder, Fig. 1, with a set of CR-39's and irradiated by the e-beam ($E = 30 \text{ kV}$, $J = 0.2\text{-}0.6 \mu\text{A/cm}^2$).

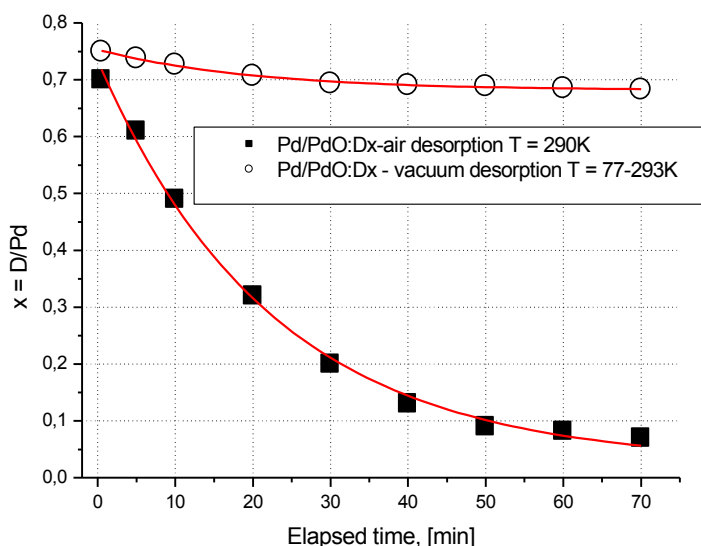


Fig.3. - D-desorption rate from the Pd/PdO:D_x samples in vacuum (electrolysis at T=280 K with cooling down to T = 77K after electrolysis termination) and in air at ambient conditions (electrolysis at T=290K). Notice very low D-desorption rate in vacuum

D-desorption from the Pd/PdO:D_x sample in vacuum without e-beam excitation and in air are shown in Fig. 3. Under e-beam excitation the desorption rate is $J_D \sim 3.3 \times 10^{15} \text{ D/s-cm}^2$. This desorption rate is consistent with the rate of D-desorption in air at ambient conditions ($\sim 2\text{-}3 \times 10^{15} \text{ D/s-cm}^2$). Results of Rutherford Back Scattering/Elastic Recoil Detection (alphas $E_\alpha = 2.2 \text{ MeV}$, depth 2 μm) (RBS/ERD profiles) of samples are presented in Fig.4.

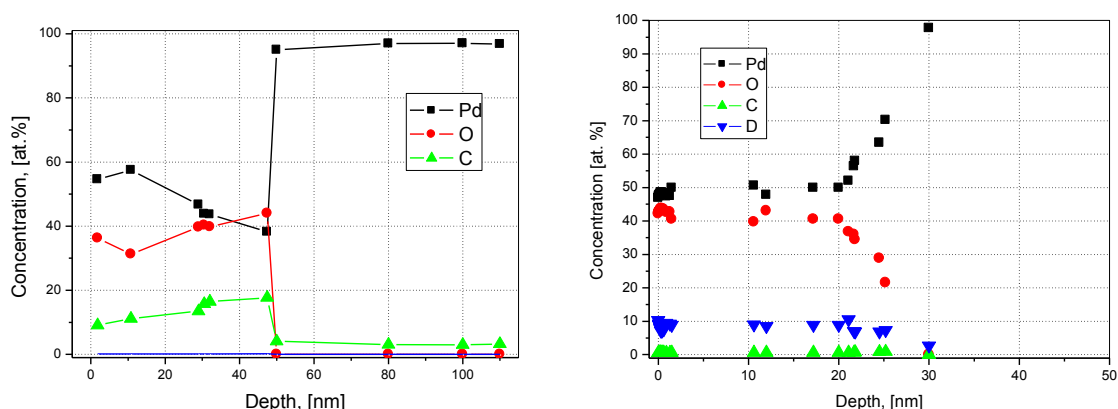


Fig.4. - RBS/ERD profiles of the Pd/PdO samples prior to D-loading –left; after electrochemical loading and D-desorption in vacuum during 50 min of e –beam ($J = 0.6 \mu\text{A/cm}^2$ $U = 30 \text{ kV}$) treatment – right

After 50 min of e-beam bombardment some moderate reduction of PdO and carbon layers is observed (from 40 to 25 nm). The residual D is located within the PdO layer. SEM measurements show that e-beam bombardment

is accompanied by formation of numerous pores (from Pd through the PdO) with diameters in the range of 100 – 2000 nm (see Fig. 5). These larger diameter pores ($\varnothing > 350$ nm) have not been found in the “blank” Pd/PdO:H_x samples after e-beam. Large craters with the $\varnothing \sim 10,000$ -12,000 nm are also present at the Pd/PdO:D_x surface after e-beam treatment.

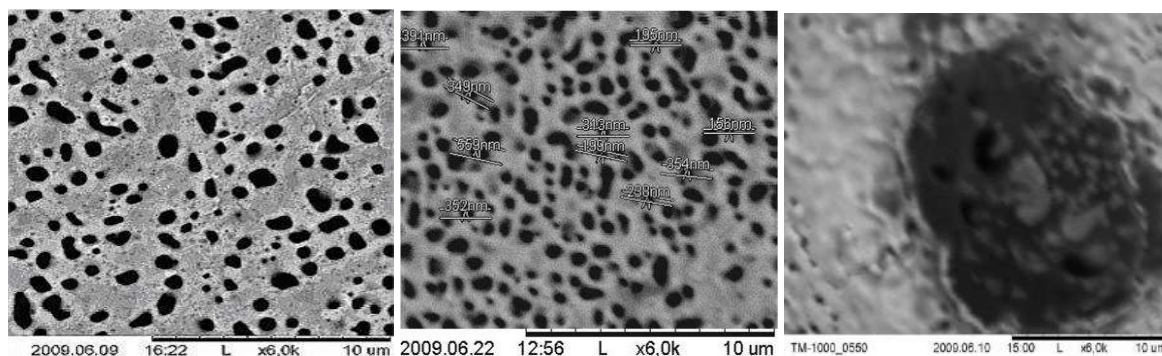


Fig.5. - SEM Pd/PdO:D_x-left and Pd/PdO:H_x-center images after electrolysis + e-beam. Notice larger diameter pore generation in Pd/PdO:D_x. Example of the $\sim 12,000$ nm diameter “crater” at the Pd/PdO:D_x surface after e-beam bombardment (right).

TiD_x samples were prepared as follows. The Ti foils, 30 and 300 μm thick, have been loaded in 1M solution of D₂SO₄ in D₂O during $t = 35$ hr at $J = 30$ mA/cm², in order to dissolve the TiO₂ oxide layer at the Ti-surface and to provide D-penetration. The average loading ($x = D/\text{Ti} = 0.1$ at depth of 2-3 μm) has been determined by weight balance. The D-desorption rate for TiD_{0.1}, from weighing before and after e-beam irradiation, is consistent with the $J_D \sim 2.0 \times 10^{14}$ D/s-cm². All desorbed deuterons in TiD are released by e-beam irradiation energy, since the chemical compound is absolutely stable at $T = 300$ K. RBS/ERD profiles of the TiD_x samples prior to e-beam bombardment –left; after D-desorption in vacuum during 60 min of e –beam are presented in Fig.6.

RBS data taken before e-beam treatment show the presence of a TiO₂ oxide layer at the surface down to 150 nm. After e-beam excitation the stoichiometry of the Ti oxide changes toward reduction of oxygen (TiO_{0.1}). The O-depth does not change. The X-ray spectrum shows almost complete oxide reduction. Estimates of D-desorption rate from TiD_x using RBS data before and after e-beam gives $v(D) = 1.5 \times 10^{14}$ D/s-cm², which is 20 times lower than $v(D)$ in Pd/PdO:D_x. The pore size is very small. Some large diameter craters ($\varnothing > 10$ μm) appear at the TiD_x surface after both e-beam and X-ray irradiation.

2. Charged Particle Detection and Identification

Background measurements show that there are no proton and alpha emission effects without e-beam stimulation (see Fig's. 7 and 8).

Cumulative results with Background subtracted for 4 series of runs (total time of e-beam exposure = 3300 min) are presented in Fig. 9. Peak positions are shifted with increasing of shielding thickness. Left peak is accompanied with 3-MeV protons, other peaks – with alpha-particles with energies 10 – 20 MeV.

Reproducibility of results is illustrated by Fig.10: The number of counts in the 3 MeV peak is roughly proportional to the cumulative exposure time of detectors 1 and 2 to Pd/PdO:D_x samples under e-beam.

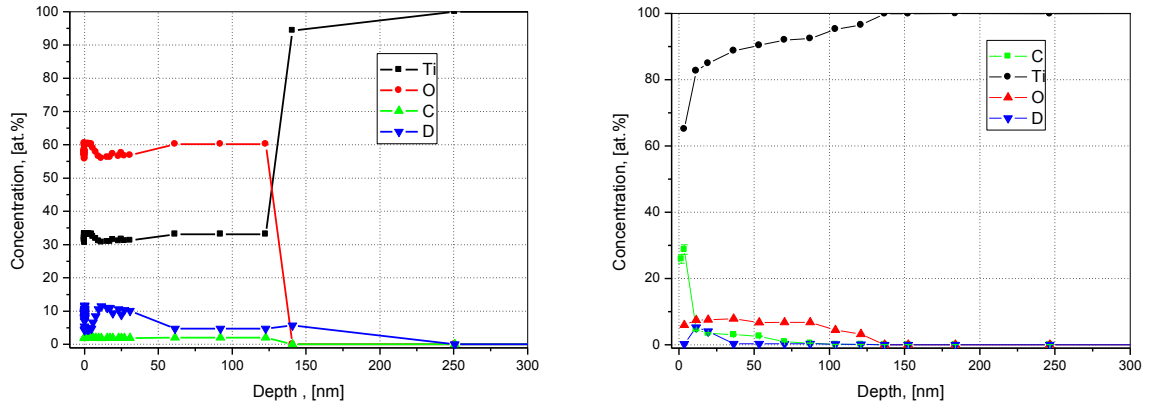


Fig.6. - RBS/ERD profiles of the TiD_x samples prior to e-beam bombardment –left; after D-desorption in vacuum during 60 min of e –beam ($J=0.6 \mu A/cm^2$ $U = 30$ kV) treatment - right

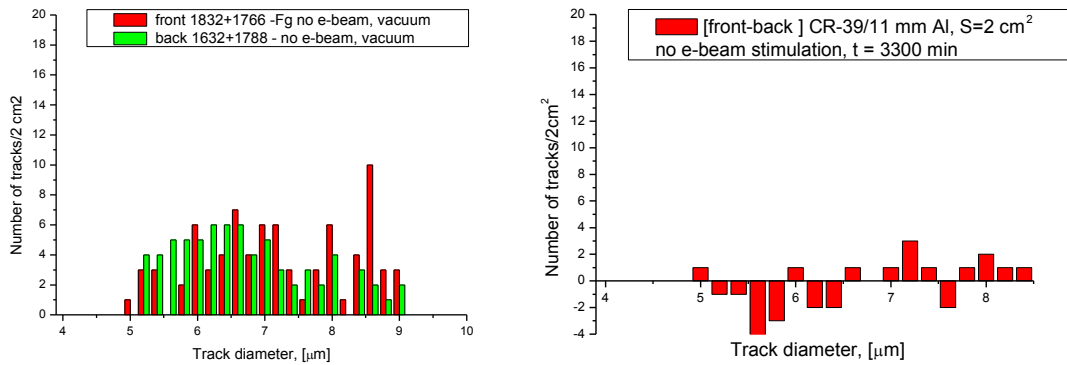


Fig.7. - Track diameter distributions for Pd/PdO: D_x without e-beam stimulation: no proton and alpha effects: CR-39/11 μm Al filter (4 samples, $t = 3300$ min). Front and back sides of detector (left). Difference of front and back sides of detector (right).

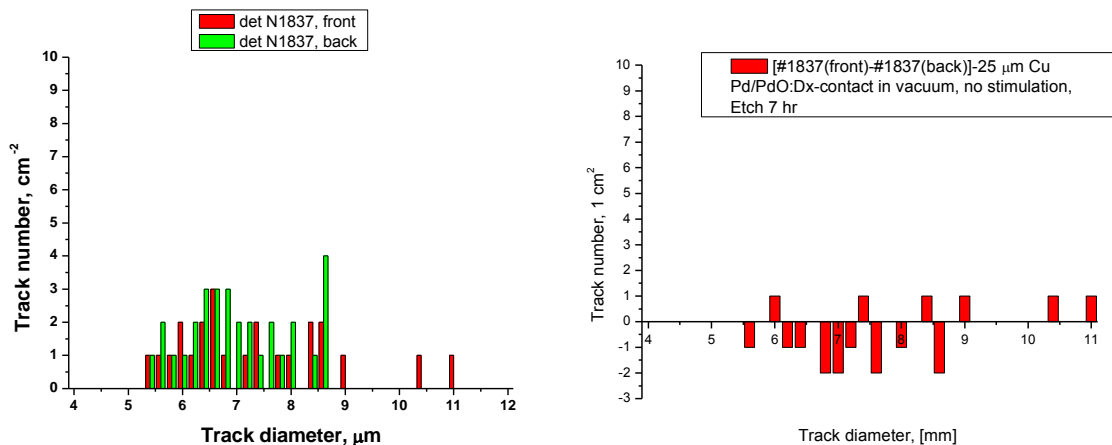


Fig.8. - Track diameter distributions for Pd/PdO: D_x without e-beam stimulation: no proton and alpha effects: 25 μm Cu covered CR-39 (4 samples, $t = 3300$ min). Front and back sides of detector (left). Difference of front and back sides of detector (right).

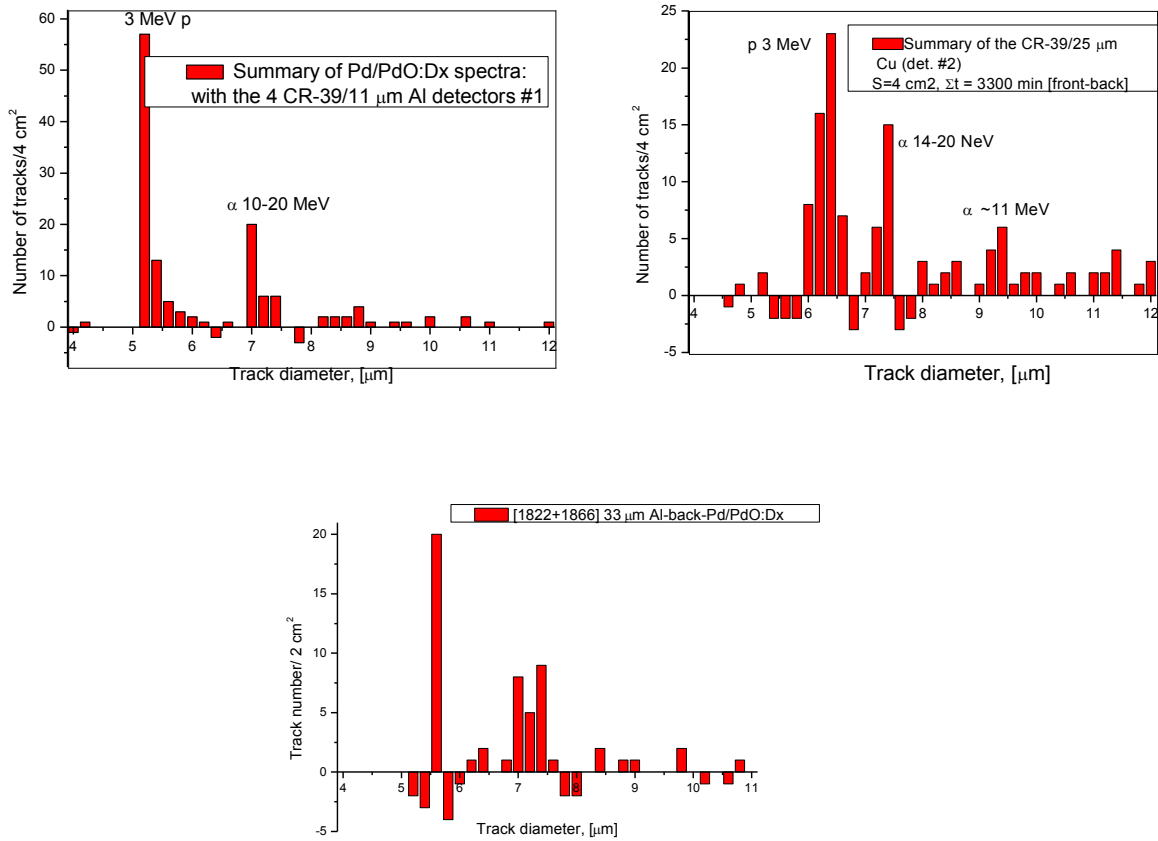


Fig. 9. - Total result with Background subtracted: Sums for 4 series of runs ($\Sigma t = 66 \times 50$ min, $S = 4$ cm² for #1 and #2): (11 μm Al)- left; (25 μm Cu)- right; the det. #3-below: $S = 2$ cm², $t = 1800$ min (33 μm Al). Notice shift of 3 MeV proton peak in these 3 detectors

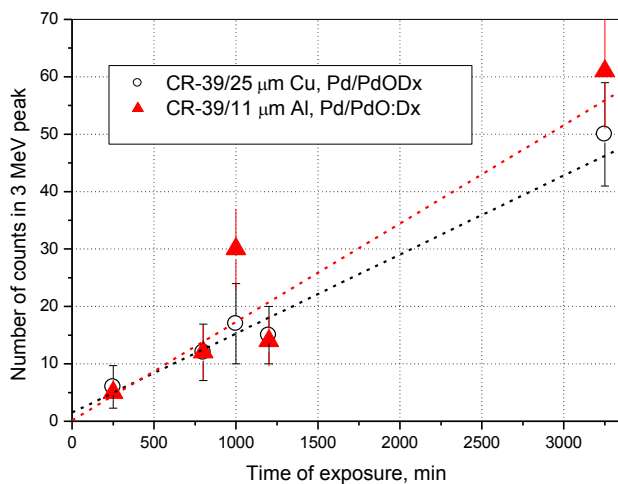
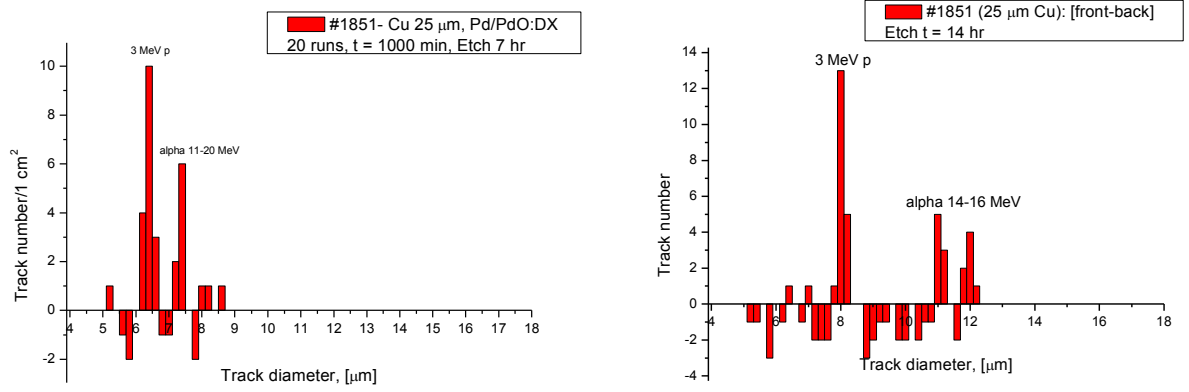


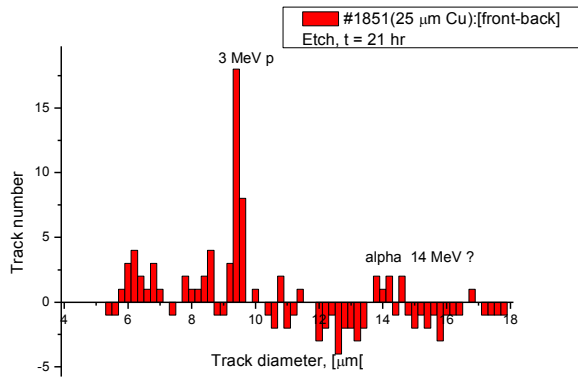
Fig. 10. - Reproducibility: The number of counts in 3 MeV peak is roughly proportional to the time of detectors 1 and 2 exposure with the Pd/PdO:D_x samples under e-beam

Additional proof of the correctness of the identification and energy of observed charged particles is obtained by successive etching of the CR-39 detectors (Fig.11) and comparing the diameters at various depths with the calibration curves (Fig.2).

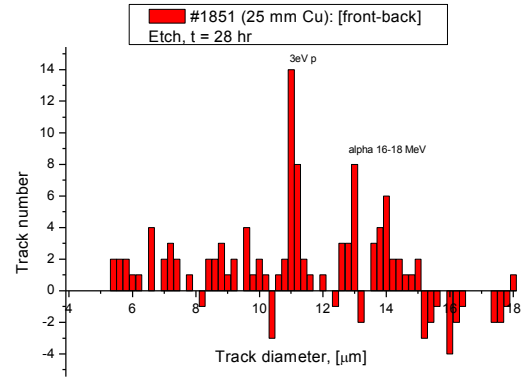


a)

b)



c)



d)

Fig. 11. - Differential spectra (with the subtracting of the rear face results) of #1851 CR-39/25 μm Cu filtered detector #2 after its etching during 7 (a), 14(b), 21(c) and 28(d) hr.

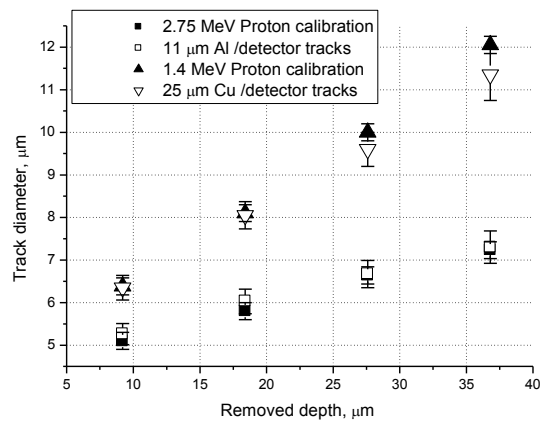


Fig. 12. - Track diameter vs. removed depth (d(h)) for “proton” tracks detected during sequential etching of the detectors 1 and 2, respectively.

Differential spectra (Foreground minus Background) of CR-39/25 μm Cu filtered detector #2 after etching during 7,14,21 and 28 h are presented in Fig.11. The same measurements were carried out for the 11 μm Al filtered detector (data not shown).

Fig. 12 presents the dependence of track diameters for proton-like tracks on removed depth. Note that in our etching conditions the bulk etch rate is $V_B = 1.3 \mu\text{m/h}$, and every 7 h we removed $\sim 9.1 \mu\text{m}$. The black squares and triangles represent the fit of experimental tracks from detectors 1 and 2 (empty squares and triangles, respectively) with $d(h)$ functions obtained using normal incidence accelerator CR-39 bombardment at proton energies 2.75 (consistent with 3 MeV proton after its passage through 11 μm thick Al foil) and 1.4 (consistent with to 3 MeV proton after its passage through the 25 μm thick Cu foil) MeV, respectively. This provides additional evidence of stimulated emission of 3-MeV proton and energetic alpha particle emissions in Pd/PdO:D_x samples.

Particle emission rates are estimated by averaging results from absorber covered CR-39 detectors (11 μm Al and 25 μm Cu) with results:

- For 3 MeV protons: $N_p = (1.12 \pm 0.12) \times 10^{-3}$ p/s-cm² of the Pd/PdO:D_x sample (significance level, $L \sim 10.0 \sigma$). The yield of DD-reaction in the Pd/PdO:D_x target under e-beam bombardment, taken only for movable deuterons) is found to be $\lambda_{DD} \sim 6 \times 10^{-19}$ p/DD-pair (4 orders of magnitude above the “Jones level”).
- For 10-20 MeV alphas $N_\alpha = (0.46 \pm 0.075) \times 10^{-3}$ α /s-cm² of the Pd/PdO:D_x sample, (significance level $L \sim 6.0 \sigma$).
- For the detector placed under the rare (non-irradiated by e-beam), position 3, side of the Pd/PdO:D_x sample: $N_p = (7.2 \pm 1.6) \times 10^{-4}$ p/s-cm² and $N_\alpha = (4.3 \pm 0.8) \times 10^{-4}$ α /s-cm² of the Pd/PdO:D_x sample.

Fig.13 presents the TiD_x e-beam stimulation results. Both statistically significant 3 MeV proton (5.2-5.4 μm track diameter) and 11-20 MeV alphas (7.0-7.6 μm track diameter) bands are found in the 11 μm Al covered detector (left); bands of 1.5 MeV protons (track diameter 6.0-6.6 μm , consistent with the 3 MeV proton losses in 25 μm Cu foil) and 14 MeV alphas (track diameter near 7.4 μm , consistent with ~ 17 MeV alpha losses in 25 μm Cu foil are detected (right). No statistically significant results have been found over all differential spectrum from the rare side of the TiD_x sample, position 3.

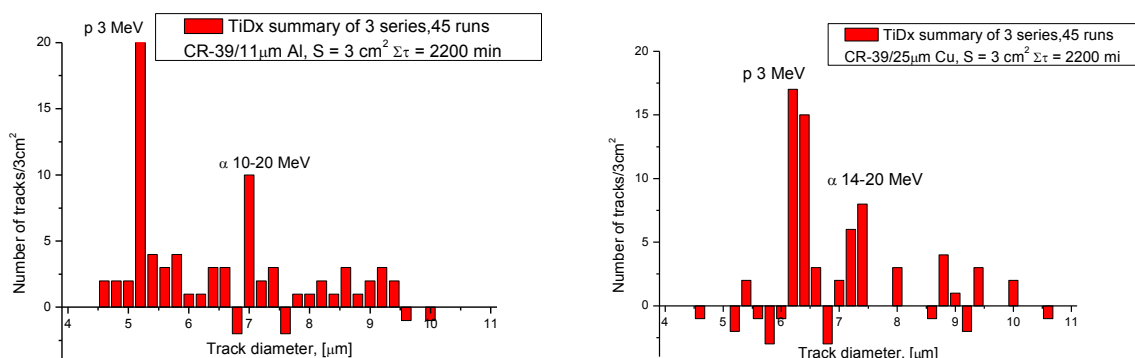


Fig.13. - TiD_x e-beam stimulation results: total 42 runs of 60 min each: two CR-39 detectors [11 μm Al (left) and 25 μm Cu (right)] with the Background (rear side) subtracting.

Average emission rates from foil covered CR-39 detectors (11 μm Al and 25 μm Cu) for 3 MeV protons and energetic alphas in TiD_x during 42 runs in 3 series ($t = 2200$ min) are:

- For 3 MeV protons: $\langle N_p \rangle = (8.4 \pm 1.5) \times 10^{-4}$ p/s-cm² of TiD_x sample (the significance level $L = 5.6 \sigma$). The yield of DD-reaction in the TiD_x target under e-beam bombardment, taken only for movable deuterons) is found to be $\lambda_{DD} \sim 5 \times 10^{-18}$ p/DD-pair (6 orders of magnitude above the “Jones level”).

- For 10-20 MeV alphas $\langle N_\alpha \rangle = (4.7 \pm 1.0) \times 10^{-4}$ α/s-cm² of the TiD_x sample, (the significance level $L \sim 4.5\sigma$). The soft component of α (E ~ 11 MeV) is not statistically significant from the non-irradiated by e-beam face of the TiD_x sample.

4. Discussions

DD-reaction rate in the Pd/PdO:D_x

A simple model of the experiment will be used to estimate the DD-reaction rate in the Pd/PdO:D_x target under electron bombardment. The e-beam stimulated D-desorption flux moving toward the Pd/PdO:D_x surface will be treated as a low energy projectile or “deuteron beam”. The deuterated surface of the Pd/PdO sample is treated as deuterium “target”. The deuteron (D⁺) “current”, is estimated from D-desorption rate, $J_d = 0.5$ mA/cm². The mean concentration of target is estimated from the mean D/Pd ratio during e-beam bombardment ($\langle x \rangle \sim 0.15$ or $N_d = 1.1 \times 10^{22}$ cm⁻³). The thick target yield I_{DD} is computed from:

$$I_{DD} = J_d N_{\text{eff}}(T) \times \int_0^{E_d} f(E) \sigma_{DD}(E) (dx/dE) dE$$

Here J_d – deuteron current density; $N_{\text{eff}}(T)$ – effective concentration of non-free D in metal at temperature T , captured at depth x : ($N_{\text{eff}}(T) = N_0 \exp(-\varepsilon_d \Delta T / k_B T T_0)$, where N_0 is the D concentration at $T_0 = 290$ K; $f(E)$ – enhancement factor [$f(E) = Y_{\text{exp}}(E) / Y_b(E) = \exp[\eta \pi(E) U_e / E]$]; σ_{DD} – is the bare DD- cross-section; dx/dE – is the stopping power in target calculated with Monte-Carlo code SRIM [4].

The deuteron screening potential U_e can be determine using the formula: $U_e = (T/T_0)^{-1/2} [a \ln(y) + b]$ [2] - an empirical equation obtained from the analysis of accelerator data for 70 elements of periodic Table (the data by Raiola et al [3]): where $a = 145.3$ and $b = 71.2$ – are numerical constants; $y = k y_0 (J_d / J_0)$, with $k = \exp(-\varepsilon_d \Delta T / k_B T T_0)$, $y_0 = \text{Pd/D ratio at } T_0 = 290 \text{ K}$, and $J_0 = 0.03 \text{ mA/cm}^2$. Substitution of $J_d = 0.5 \text{ mA/cm}^2$, $T = 290 \text{ K}$ and $\langle \text{Pd/D} \rangle = 6.7$ in eq. for U_e gives $U_e = 730 \pm 50 \text{ eV}$. This screening value falls roughly into the interval limited by Kasagi’s (600 eV for Pd/PdO [5]) and Raiola’s (800 eV for Pd [3])

The DD-reaction rate of ~ 0.001 p/s-cm² in 4π ster. could be reached in the Pd/PdO:D_x target (taking into account $U_e \sim 730$ eV) only if the mean kinetic energy of the desorbing deuterons is of the order of $\langle E_d \rangle \sim 3-4$ eV. In contrast, if the mean deuteron energy $\langle E_d \rangle \sim kT$, with the same U_e , the DD-reaction rate would be only $\sim 10^{-7}$ p/s-cm², or well below our detection limit. This result strongly supports the theoretical prediction [1] with regards to electron excitation of hydrogen subsystem in Pd deuteride (hot deuteron generation). The 3-4 eV deuteron flux claim serves as an evidence for the generation of a strong electric field ($\sim 10^8$ V/cm) on a scale of the lattice parameter ($a_0 = 0.39$ nm) due to plasmon formation in this experiment.

TiD_x DD-reaction rate

Taking $J_d = 0.03 \text{ mA/cm}^2$ and $y_0 \sim 2.0$ (the surface D-concentration is $x = \text{D/Ti} \sim 0.3$ during e-bombardment) one can obtain $U_e \sim 130$ eV. At this small screening potential, in order to produce DD-reaction rate of the order of ~ 0.001 p/s-cm², the kinetic energy of deuteron flux (in laboratory system) has to be rather higher ($E_d \sim 500$ eV). This high kinetic energy can be gained by D⁺ acceleration in a strong electric field created by electrostatic charging of the TiO₂ surface with e-beam.

(E_d)_{eff} = $\varepsilon_0 + e E(\text{TiO}_2) x h(\text{TiO}_2)$. At $\varepsilon_0 \sim 3$ eV (the initial kinetic energy of D⁺ in Ti caused by plasmon generation), $E(\text{TiO}_2) \sim 3.5 \times 10^7$ V/cm (electrical strength of TiO₂) and $h(\text{TiO}_2) = 1.5 \times 10^{-5}$ cm, the (E_d)_{max} ~ 500 eV(!!!) suggesting D⁺ acceleration by a strong electric field during deuteron drift and diffusion through the Ti oxide.

5. Conclusions

- The vacuum experiments with and without e-beam irradiation, lead to the conclusion that an electron beam ($J \sim 100\text{-}300$ nA, $E = 30$ keV) stimulus of the Pd and Ti deuterided targets (cathodes) surface can enhance the intensity of the emissions of nuclear charged particles.
- Both products of DD-reaction (3 MeV) protons and high energy alphas (11-20 MeV) are clearly identifiable in e-beam stimulation experiment with the Pd/PdO:D_x and TiD_x targets.
- Signatures of 3 MeV protons and energetic alphas appear on the surface of all (2 or 3) independent detectors in the same experiment covered by metallic foil filters with different stopping ranges/powers.
- The data analysis on the Pd/PdO:D_x target supports reasonable estimates of DD-reaction cross sections and the enhancement factors to a very low deuteron energy ($E_d \sim 3.0$ eV). Extrapolation of DD-reaction cross section and the enhancement factor with a reasonable screening potential $U_e = 730$ eV, satisfactorily accounts for the detected DD-reaction rate in these experiments. This calculation and the underlying data strongly support the theoretical prediction [1] with regard to electron excitation of hydrogen subsystem in Pd deuteride.
- In order to enhance charged particle yield, we plan to vary target deuterides, as well as the current and energy of electron beam. These optimization studies will bring understanding of the possible technological value of e-beam and other excitation.
- More work also should be done with respect to the energy spectra characterization and the origin of the energetic alpha emission.

6. References

- [1]. V.M., Silkin, I.P Chernov et al, Phys. Rev., B **76**, 245105 (2007)
- [2]. A. Lipson et al, High Energy Chem. **42**(4), 319 (2008)
- [3]. F. Raiola et al, Europhys. J., **A19**, 283 (2004)
- [4]. J.F. Ziegler and J.P. Biersack, code SRIM 2003
- [5]. Yuki H., Kasagi J., Lipson A. G. et al // JETP Lett. 1998. v. **68**(11). p. 785-790.